

Federated Multi-Task Clustering

Suyan Dai, Gan Sun*, Member IEEE, Fazeng Li, Xu Tang, Qianqian Wang, and Yang Cong Member, IEEE

Abstract—Spectral clustering has emerged as one of the most effective clustering algorithms due to its superior performance. However, most existing models are designed for centralized settings, rendering them inapplicable in modern decentralized environments. Moreover, current federated learning approaches often suffer from poor generalization performance due to reliance on unreliable pseudo-labels, and fail to capture the latent correlations amongst heterogeneous clients. To tackle these limitations, this paper proposes a novel framework named **Federated Multi-Task Clustering** (*i.e.*, FMTC), which intends to learn personalized clustering models for heterogeneous clients while collaboratively leveraging their shared underlying structure in a privacy-preserving manner. More specifically, the FMTC framework is composed of two main components: client-side personalized clustering module, which learns a parameterized mapping model to support robust out-of-sample inference, bypassing the need for unreliable pseudo-labels; and server-side tensorial correlation module, which explicitly captures the shared knowledge across all clients. This is achieved by organizing all client models into a unified tensor and applying a low-rank regularization to discover their common subspace. To solve this joint optimization problem, we derive an efficient, privacy-preserving distributed algorithm based on the Alternating Direction Method of Multipliers, which decomposes the global problem into parallel local updates on clients and an aggregation step on the server. To the end, several extensive experiments on multiple real-world datasets demonstrate that our proposed FMTC framework significantly outperforms various baseline and state-of-the-art federated clustering algorithms.

Index Terms—Federated learning, unsupervised learning, spectral clustering, multi-task learning, tensor methods.

I. INTRODUCTION

SPECTRAL clustering [1] is a powerful and fundamental algorithm that has demonstrated state-of-the-art performance in numerous applications. It operates by effectively discovering high-quality embeddings from the manifold structure inherent in the data distribution. Recent research has extended the boundaries of spectral clustering to more complex scenarios. For example, researchers have proposed various scalable variants [2], [3] to address computational challenges. To learn more discriminative feature representations from raw data, deep spectral clustering improves clustering performance

Suyan Dai, Gan Sun, Fazeng Li and Yang Cong are with the School of Automation Science and Engineering, South China University of Technology, Guangzhou 510641, China. (email: 18790457702@163.com, sungan1412@gmail.com, lifazeng818@gmail.com, congyang81@gmail.com)

Xu Tang is with the School of Software, Dalian University of Technology, Dalian City 116024, China. (email: tangxu@mail.dlut.edu.cn)

Qianqian Wang is with the School of Telecommunications Engineering, Xidian University, Xi'an, 710071, China.(email: qqwang@xidian.edu.cn)

This work is supported by the National Key Research and Development Program of China (2022YFC2806101) and National Nature Science Foundation of China under Grant (62273333, 62225310, 62127807), and the Fundamental Research Funds for the Central Universities (2024ZYGXZR024).

*The corresponding author is *Prof. Gan Sun*.

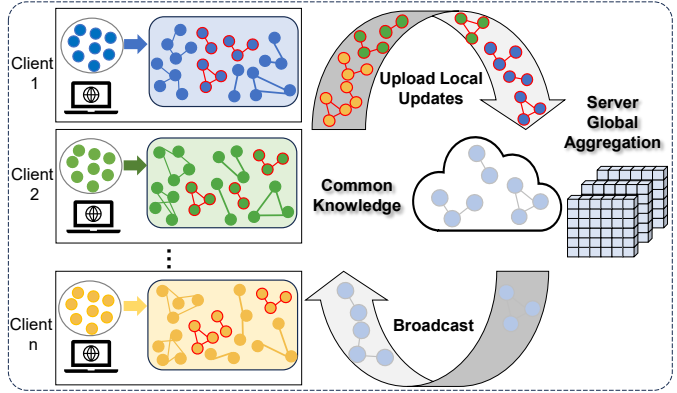


Fig. 1. Motivation of our federated multi-task clustering model, where clients in each round share local model updates and the server aggregates these into a model tensor with multi-task constraint, distilling shared structure which is then broadcast back to refine each personalized model.

through the organic integration of deep neural networks and spectral analysis [4], [5]. However, most existing spectral clustering algorithms rely on a critical assumption: data can be freely collected and processed by a central server. This centralized requirement renders them inapplicable when data is distributed across different institutions or user devices due to privacy constraints. Consequently, how to adapt the principles of federated learning to clustering methods has emerged as a novel paradigm.

Federated learning (FL) [6] has emerged as a prominent distributed paradigm, enabling collaborative model training while preserving data privacy. In the context of unsupervised federated clustering, most existing works [7], [8] have largely adopted strategies from the broader FL field. These strategies typically involve either aggregating local clustering results into a unified global model [9]–[11], or adopting personalized approaches to learn distinct models for different clients [12], [13]. However, these methods often fail to adequately account for the underlying relationships that exist among clients within the same clustering context. For example, in cross-institution web page clustering (*e.g.*, the WebKB dataset), while the data distribution of each university (client) is distinct, requiring a personalized solution, they simultaneously share an underlying semantic structure (*e.g.*, "Faculty page" and "Course page"). An advanced federated clustering method that can both learn personalized models and precisely capture this shared structure would significantly enhance performance across all tasks.

Inspired by the aforementioned observations, we in this paper propose a novel federated clustering learning framework, which takes two types of relations into consideration: 1) **Intra-client Correlation**, which refers the correlations amongst

heterogeneous data in each client, and the process of learning cluster labels. In contrast, most existing federated clustering methods rely heavily on unreliable pseudo-labels for training and struggle with out-of-sample generalization; and 2) **Inter-client Correlation**, the latent common knowledge should be consistent among heterogeneous clients, which resolves the limitation that the majority of existing federated clustering methods. For example, in the 20NewsGroups dataset, each client owns articles from different thematic forums. These corpora follow non-overlapping vocabularies and discourse styles, so collapsing them into a single spectral model erases crucial client-specific cues. Yet they still share latent communicative patterns, which FMTC captures through its tensor regularizer while retaining personalized projections for every forum.

To tackle these dual challenges, as shown in Fig. 1, we propose a Federated Multi-Task Clustering (*i.e.*, FMTC), which can achieve federated clustering knowledge transfer among heterogeneous clients. To achieve this goal, two components of our FMTC model are proposed to preserve the common information among multiple clients, *i.e.*, client-side personalized clustering module and a server-side tensorial correlation module. To be specific, the personalized clustering module in each client integrates the spectral embedding learning and the mapping function optimization into a unified closed-loop system, which can capture the intrinsic manifold structure of the local client data, and be able to out-of-sample data. Based on the assumption that multiple client models are lie within a shared global subspace, the server-side tensorial correlation module mathematically organizes the local model parameters from all clients into a third-order tensor, and apply a low-rank regularization to constrain inter-client correlation. This module could effectively filter out client-specific noise while enforcing a global consensus on the model structure, thereby allowing the shared knowledge to reinforce the performance of each individual client. To solve this optimization problem, we derive an efficient and privacy-preserving distributed algorithm based on the Alternating Direction Method of Multipliers (ADMM). This algorithm decomposes the complex global objective into parallel local updates on clients and a global aggregation step on the server, ensuring convergence without exchanging raw data. To the end, our FMTC model is evaluated against several spectral clustering algorithms and federated clustering learning models on several datasets. The experimental results strongly support our proposed FMTC model.

Our main contributions are summarized as follows:

- We propose a Federated Multi-Task Clustering (*i.e.*, FMTC) framework, which uniquely bridges the gap between personalized local adaptation and global collaboration, effectively resolving the dual challenges of unreliable pseudo-label dependency within clients and the neglect of structural correlations among clients.
- We design a novel bi-level collaborative strategy that seamlessly integrates the client-side personalized clustering module with the server-side tensorial correlation module. This design allows for the direct learning of robust mapping functions for out-of-sample inference while explicitly capturing the high-order shared knowledge across heterogeneous clients via low-rank tensor

regularization.

- We develop a privacy-preserving distributed optimization algorithm based on ADMM to solve the distinct nonconvex joint problem efficiently. Extensive experiments on seven benchmarks validate that FMTC outperforms state-of-the-art methods, particularly in scenarios requiring strong generalization capabilities on unseen data.

The remainder of this paper is organized as follows. Section II reviews the related literature on spectral clustering and federated clustering. Section III details the proposed FMTC framework, including the mathematical formulation of the local and global objectives, followed by the distributed ADMM optimization algorithm in Section IV. Section V presents the experimental results and Section VI concludes the paper and discusses future research directions.

II. RELATED WORK

In this section, we review the literature relevant to our work with two main streams: Spectral Clustering and Federated Clustering, and discuss the recent advancements in these fields.

A. Spectral Clustering

Spectral clustering is a powerful graph clustering technique, widely applied for its ability to effectively identify non-convex clusters and reveal the intrinsic manifold structure of the data [1]. Its success is particularly notable in various multimedia applications, such as image segmentation, video object clustering, and community detection in social networks. As the field matured, research has focused on advancing its core components. One line of work has concentrated on the construction of similarity graphs, leading to the development of adaptive neighbor selection techniques and local density-sensitive similarity measures to create more robust graph representations [2], [14]. Another direction explores variants of the Laplacian matrix itself to better capture the local manifold structure of the data [15], [16]. To improve applicability for large-scale data, significant efforts have been made in developing approximation methods to improve computational efficiency [3], [17]. Furthermore, the integration of deep learning has led to deep spectral clustering, which uses neural networks to learn an optimal embedding space prior to spectral analysis [4], [18]. Despite this rich body of work advances its different components, a common characteristic of these models is their centralized design. The execution of the algorithm requires unrestricted access to the entire dataset. This property poses a significant challenge for applications in distributed scenarios with strict privacy and data sovereignty requirements.

B. Federated Clustering Learning

Research on clustering in federated learning [6] can be broadly divided into two categories. The first category uses clustering as an auxiliary tool for handling non-independent and identically distributed (Non-IID) data, with the primary goal of improving the performance of downstream supervised learning tasks [19], [20]. In these approaches, the system typically groups clients (or devices) to train more adaptive supervised models for each group [21]–[23]. The second category

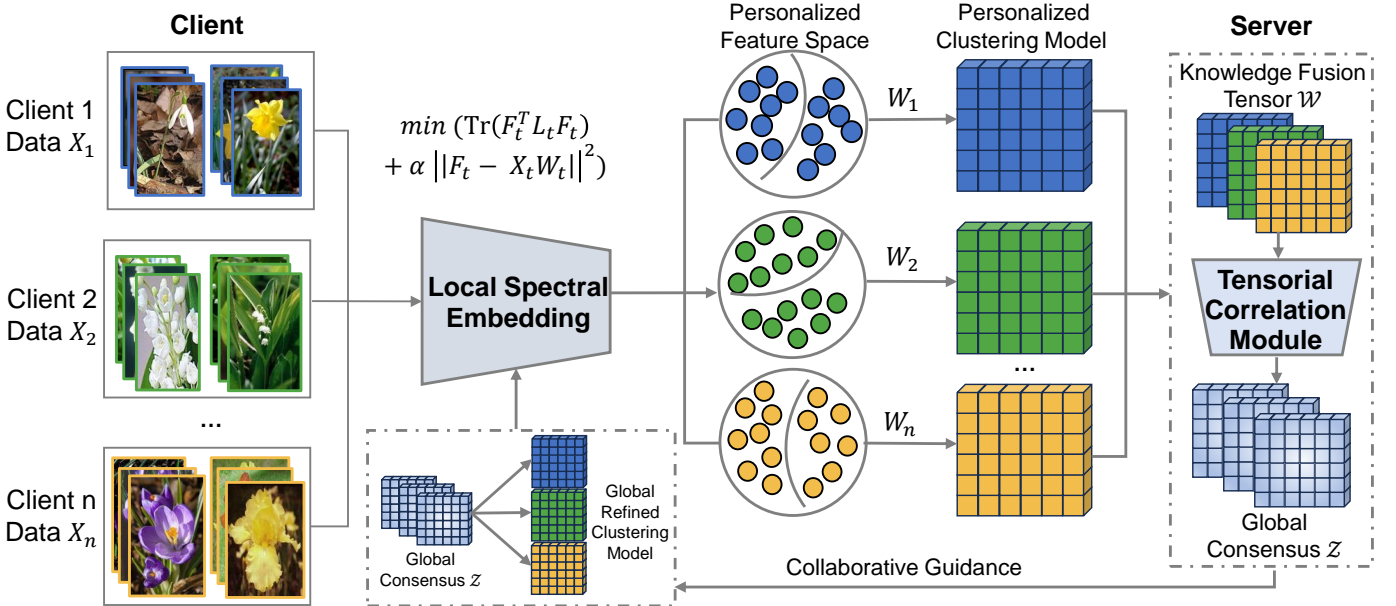


Fig. 2. The architecture of our Federated Multi-Task Clustering (FMTC) framework, where the process begins with heterogeneous data samples $\{X_t\}$ from diverse clients. At the client level, each client data is processed through Local Spectral Embedding, which is optimized according to our local objective function. This process generates a client-specific Personalized Feature Space and learns a corresponding Personalized Clustering Model W_t . At the server level, all personalized clustering models $\{W_t\}$ are collected and stacked into a Knowledge Fusion Tensor \mathcal{W} . The Tensorial Correlation Module is then applied to this tensor to distill a Global Consensus \mathcal{Z} , representing the shared knowledge across all tasks. This consensus is further used to obtain the Global Refined Clustering Model. Finally, the Collaborative Guidance from the server provides regularization back to the local spectral embedding, completing the federated optimization loop.

focuses directly on the unsupervised clustering task itself [24]. This line of research aims to find meaningful cluster structures from distributed data while preserving privacy. Such methods hold great promise for multimedia scenarios, for instance, in building personalized media recommendation systems or analyzing user behavior across different platforms without sharing raw data. Common technical approaches include the iterative aggregation of local models or parameters, such as in Federated K-Means [9], [10], and methods based on distributed matrix factorization [25], [26]. However, a common limitation persists across both categories of existing federated clustering methods. They typically stop at learning either a single global model or a set of independent personalized models, failing to explicitly model the underlying deep relationships between clients as a core component of the framework. To the best of our knowledge, there are no existing works that simultaneously learn personalized models and explicitly capture global task relationships within a unified federated clustering setting. Our work aims to fill this critical gap by introducing a multi-task learning paradigm, representing the first effort to achieve federated multi-task clustering.

III. OUR PROPOSED METHOD

A. Preliminaries

Given a data set of n points with dimensions d , $\mathbf{X} = [\mathbf{x}_1, \dots, \mathbf{x}_n] \in \mathbb{R}^{d \times n}$, the clustering task in each client aims to partition these points into c groups. Spectral clustering [1] constructs a similarity graph to encode pairwise relationships as a similarity graph. The structure of the graph is captured by a weighted adjacency matrix $\mathbf{A} \in \mathbb{R}^{n \times n}$, where $A_{ij} > 0$

quantifies the affinity between points \mathbf{x}_i and \mathbf{x}_j . A common construction method is the graph of the k -nearest neighbor (k -NN), where edge weights are defined by a Gaussian kernel:

$$A_{ij} = \begin{cases} e^{-\frac{\|\mathbf{x}_i - \mathbf{x}_j\|^2}{2\sigma^2}} & \text{if } \mathbf{x}_i \in \mathcal{N}_k(\mathbf{x}_j) \vee \mathbf{x}_j \in \mathcal{N}_k(\mathbf{x}_i) \\ 0 & \text{otherwise,} \end{cases} \quad (1)$$

and $\mathcal{N}_k(\cdot)$ is the set of k -nearest neighbors and σ is the kernel bandwidth. We can compute the diagonal degree matrix \mathbf{D} from \mathbf{A} , where $D_{ii} = \sum_j A_{ij}$. The unnormalized Laplacian graph is then defined as $\mathbf{L} = \mathbf{D} - \mathbf{A}$. For improved numerical stability and its connection to the Normalized Cut objective, we use the symmetric normalized Laplacian $\hat{\mathbf{L}}$:

$$\hat{\mathbf{L}} = \mathbf{D}^{-1/2} \mathbf{L} \mathbf{D}^{-1/2} = \mathbf{I} - \mathbf{D}^{-1/2} \mathbf{A} \mathbf{D}^{-1/2}. \quad (2)$$

The final objective of spectral clustering is to find a discrete partition of the data. This can be formally expressed as an optimization problem to find an indicator matrix $\mathbf{Y} \in \mathbb{R}^{n \times c}$, where c is the number of clusters. The problem can be formulated as:

$$\min_{\mathbf{Y}} \text{Tr}(\mathbf{Y}^\top \hat{\mathbf{L}} \mathbf{Y}) \quad \text{s.t. } \mathbf{Y} \in \text{Idx}, \quad (3)$$

where the set Idx is the set of all valid partition matrices.

Problem Definition: Our work considers a federated learning scenario consisting of a central server S and m clients $\{C_t\}_{t=1}^m$. The data is distributed across these clients, where each client C_t holds a local dataset $\mathbf{X}_t \in \mathbb{R}^{n_t \times d_t}$. Here, n_t is the number of local samples and d_t is the feature dimensionality for client t . We formulate the clients as distinct yet correlated tasks within a multi-task Learning paradigm [27].

The server S is responsible for coordinating the clients to collaboratively learn their respective clustering structures without direct access to their local data. Our method aims to learn a distinct and high-quality clustering for each client from the decentralized local data, while leveraging shared knowledge across clients in a privacy-preserving manner. We consider a setting where all the clients share a common feature space although the number of samples n_t can vary across clients, *i.e.*, the feature dimensionality $d_t = d$ for all clients t . This is a common setting in cross-silo federated learning [28], [29].

B. Federated Multi-Task Clustering

Our Federated Multi-Task Clustering (FMTC) framework, whose overall architecture is depicted in Fig. 2, consists of two core components: local model training conducted by each client and a global objective to ensure consistency and knowledge sharing, coordinated by the server.

1) *Client-Side Personalized Clustering Module*: For the client-side personalized clustering module, the primary objective is to perform clustering on its local data \mathbf{X}_t . Existing federated solutions [30], [31] often resort to generating static pseudo-labels to train a secondary classifier, but this “two-stage” process suffers from severe error propagation. Moreover, traditional spectral clustering is non-parametric, yielding only embeddings \mathbf{F}_t defined on specific training points, which makes out-of-sample inference impossible. To address the intra-client challenge regarding the reliance on unreliable pseudo-labels and poor generalization performance, we redesign the local learning objective in each client.

Our client-side personalized clustering module proposes to learn a parametric projection matrix $\mathbf{W}_t \in \mathbb{R}^{d_t \times k}$ simultaneously with the spectral embeddings. We posit that the ideal embedding \mathbf{F}_t can be approximated by a linear transformation of the data \mathbf{X}_t . By enforcing the constraint $\|\mathbf{F}_t - \mathbf{X}_t \mathbf{W}_t\|_F^2$, we couple the manifold discovery and the mapping function learning into a unified optimization process. This design ensures that \mathbf{W}_t directly captures the intrinsic data structure without needing noisy pseudo-labels, enabling the model to robustly generalize to unseen data. The unified local objective is formulated as:

$$\begin{aligned} \min_{\mathbf{F}_t, \mathbf{W}_t} \quad & \text{Tr}(\mathbf{F}_t^T \hat{\mathbf{L}}_t \mathbf{F}_t) + \alpha \|\mathbf{F}_t - \mathbf{X}_t \mathbf{W}_t\|_F^2 \\ \text{s.t.} \quad & \mathbf{F}_t^T \mathbf{F}_t = \mathbf{I}, \end{aligned} \quad (4)$$

where the hyperparameter α controls the trade-off between preserving the ideal spectral structure (the first term) and ensuring that this structure is faithfully captured by a linear model.

2) *Server-Side Tensorial Correlation Module*: The server-side tensorial correlation module of our framework is designed to tackle the inter-client challenge, where existing methods fail to leverage the latent correlations among heterogeneous clients. We hypothesize that while local models $\{\mathbf{W}_t\}$ are personalized to distinct data distributions, they share a common underlying structure governed by the semantic nature of the tasks [32], [33].

To explicitly model this relationship, the server-side tensorial correlation module organizes the collection of local

models into a third-order tensor $\mathbf{W} \in \mathbb{R}^{d \times k \times m}$. Unlike simple parameter averaging, we impose a low-rank constraint on \mathbf{W} to capture the high-order correlations across clients. This tensor-based regularization [34] acts as a global knowledge sharing mechanism: it filters out client-specific noise and distills the shared structural knowledge into a common low-dimensional subspace. This ensures that the learning of each client is supported by the collective wisdom of all tasks. The global regularization term is defined as:

$$\begin{aligned} \min_{\{\mathbf{W}_t\}_{t=1}^m, \mathbf{W}} \quad & \beta \|\mathbf{W}\|_{S_p}^p \\ \text{s.t.} \quad & \mathbf{W}_{::,t} = \mathbf{W}_t, \quad \forall t \in \{1, \dots, m\} \end{aligned} \quad (5)$$

where β is a hyperparameter that controls the strength of the collaboration. A larger β forces the client models to be more similar, while a smaller β allows for greater personalization. This term, managed by the server with access to all $\{\mathbf{W}_t\}$, forms the core of our collaborative learning strategy.

3) *Overall Objective Function*: By combining the local client objectives (Eq. (4)) and the global collaboration regularizer (Eq. (5)), we can formulate the complete optimization problem for our FMTC framework as follows:

$$\begin{aligned} \min_{\{\mathbf{F}_t\}, \{\mathbf{W}_t\}} \quad & \sum_{t=1}^m \omega_t \left(\text{Tr}(\mathbf{F}_t^T \hat{\mathbf{L}}_t \mathbf{F}_t) + \alpha \|\mathbf{F}_t - \mathbf{X}_t \mathbf{W}_t\|_F^2 \right) \\ & + \beta \|\mathbf{W}\|_{S_p}^p \\ \text{s.t.} \quad & \mathbf{F}_t^T \mathbf{F}_t = \mathbf{I}, \end{aligned} \quad (6)$$

where \mathbf{W} is the tensor formed by stacking $\{\mathbf{W}_t\}$. This joint optimization problem is challenging to solve directly in a federated setting. The primary difficulty lies in the coupling introduced by the tensor norm regularizer $\beta \|\mathbf{W}\|_{S_p}^p$, which depends on the parameters $\{\mathbf{W}_t\}$ of all clients simultaneously. This prevents clients from optimizing their local objectives in a fully parallel and independent manner.

IV. MODEL OPTIMIZATION FRAMEWORK

To decouple the interdependent tensor constraints, we employ an alternate direction method of multipliers with variable splitting: we introduce a global auxiliary variable $\mathbf{Z} \in \mathbb{R}^{d \times k \times m}$, which serves as a “consensus” copy of the model tensor \mathbf{W} . We then enforce the constraint that the local models must agree with this global consensus, *i.e.* $\mathbf{W}_t = \mathbf{Z}_t$ for each client t , where \mathbf{Z}_t is the t -th slice of \mathbf{Z} . This allows us to reformulate Eq. (6) into an equivalent, constrained form that is separable:

$$\begin{aligned} \min_{\{\mathbf{F}_t\}, \{\mathbf{W}_t\}, \mathbf{Z}} \quad & \sum_{t=1}^m \omega_t \left(\text{Tr}(\mathbf{F}_t^T \hat{\mathbf{L}}_t \mathbf{F}_t) + \alpha \|\mathbf{F}_t - \mathbf{X}_t \mathbf{W}_t\|_F^2 \right) \\ & + \beta \|\mathbf{Z}\|_{S_p}^p \\ \text{s.t.} \quad & \mathbf{W}_t = \mathbf{Z}_t, \quad \mathbf{F}_t^T \mathbf{F}_t = \mathbf{I}, \quad \forall t \in \{1, \dots, m\}. \end{aligned} \quad (7)$$

Notice how the problematic coupling term now only involves the global variable \mathbf{Z} , while the summation part only involves local variables $\{\mathbf{W}_t, \mathbf{F}_t\}$. This separable structure is ideal for the ADMM framework, which addresses the constraints by forming an Augmented Lagrangian.

Algorithm 1 Federated Multi-Task Clustering Framework

1: **Input:** Local datasets $\{\mathbf{X}_t\}_{t=1}^m$; number of clusters k ; hyperparameters α, β, ρ .
2: **Output:** Converged local models $\{\mathbf{F}_t^*, \mathbf{W}_t^*\}$.
3: **Initialization:**
4: Server initializes global tensors $\mathcal{Z}^0, \mathcal{Y}^0$ to zero and weights $\lambda_t^0 \leftarrow 1/m$.
5: **for** $t = 1$ to m **in parallel do**
6: Client t computes its graph Laplacian $\hat{\mathbf{L}}_t$ and initializes local models $\mathbf{F}_t^0, \mathbf{W}_t^0$.
7: **end for**
8: **while** not converged **do**
9: Server sends $\{\mathbf{Z}_t^k, \mathbf{Y}_t^k, \lambda_t^k\}$ to each client t .
10: **for** $t = 1$ to m **in parallel do**
11: Update local projection matrix \mathbf{W}_t^{k+1} per Eq. (12).
12: Update local spectral embedding \mathbf{F}_t^{k+1} per Eqs. (14)-(16).
13: Client t sends its updated \mathbf{W}_t^{k+1} back to the server.
14: **end for**
15: Server gathers $\{\mathbf{W}_t^{k+1}\}$ from all clients.
16: Update the global consensus tensor \mathcal{Z}^{k+1} via TSVT per Eq. (18).
17: Update the dual variables \mathcal{Y}^{k+1} per Eq. (19).
18: **end while**
19: **return** Final models $\{\mathbf{F}_t, \mathbf{W}_t\}$.

A. Augmented Lagrangian

To solve the constrained problem in Eq. (7), we construct its **Augmented Lagrangian** with two steps. For the set of equality constraints $\mathbf{W}_t = \mathbf{Z}_t$, we firstly introduce the corresponding set of dual variables $\{\mathbf{Y}_t\}_{t=1}^m$. For notational convenience, we can stack these matrices to form a single dual variable tensor, \mathbf{Y} . Second, we add a quadratic penalty term to improve convergence properties. The resulting augmented Lagrangian L_ρ is given by:

$$\begin{aligned} L_\rho(\{\mathbf{F}_t, \mathbf{W}_t\}, \mathcal{Z}, \mathbf{Y}) \\ = \sum_{t=1}^m \omega_t \left(\text{Tr}(\mathbf{F}_t^T \hat{\mathbf{L}}_t \mathbf{F}_t) + \alpha \|\mathbf{F}_t - \mathbf{X}_t \mathbf{W}_t\|_F^2 \right) \\ + \sum_{t=1}^m \langle \mathbf{Y}_t, \mathbf{W}_t - \mathbf{Z}_t \rangle + \sum_{t=1}^m \frac{\rho}{2} \|\mathbf{W}_t - \mathbf{Z}_t\|_F^2 + \beta \|\mathcal{Z}\|_{S_p}^p, \end{aligned} \quad (8)$$

where $\langle \cdot, \cdot \rangle$ denotes the inner product of Frobenius and $\rho > 0$ is the penalty parameter. The ADMM algorithm then proceeds by iteratively minimizing L_ρ with respect to the primary variables $\{\mathbf{W}_t\}$ and \mathcal{Z} , and then updating the dual variable tensor \mathbf{Y} by updating each slice \mathbf{Y}_t . (*Note: The nonconvex orthogonality constraint $\mathbf{F}_t^T \mathbf{F}_t = \mathbf{I}$ is handled directly within the subproblem for \mathbf{F}_t and is thus not explicitly included in the Lagrangian.*)

B. Iterative Primal-Dual Update

At each iteration $k + 1$, the algorithm proceeds as follows.

1) *Primal Minimization Stage:* The primary variables, namely $\{\mathbf{F}_t, \mathbf{W}_t\}$ and the global tensor \mathcal{Z} , are updated by minimizing the Augmented Lagrangian. We decompose this

minimization into parallelizable updates on the clients and the server.

Client-Side Updates: Each client t is responsible for updating its local variables \mathbf{W}_t and \mathbf{F}_t through alternating minimization.

a. **Update of \mathbf{W}_t :** Fixing other variables, the subproblem for \mathbf{W}_t is:

$$\begin{aligned} \min_{\mathbf{W}_t} & \left\{ \omega_t \alpha \|\mathbf{F}_t^k - \mathbf{X}_t \mathbf{W}_t\|_F^2 + \text{Tr}((\mathbf{Y}_t^k)^T \mathbf{W}_t) \right. \\ & \left. + \frac{\rho}{2} \|\mathbf{W}_t - \mathbf{Z}_t^k\|_F^2 \right\}. \end{aligned} \quad (9)$$

As an unconstrained convex problem, we find the minimum by setting the partial derivative with respect to \mathbf{W}_t to zero:

$$\begin{aligned} \frac{\partial L_\rho}{\partial \mathbf{W}_t} = & \omega_t \alpha \cdot 2 \mathbf{X}_t^T (\mathbf{X}_t \mathbf{W}_t - \mathbf{F}_t^k) \\ & + \mathbf{Y}_t^k + \rho (\mathbf{W}_t - \mathbf{Z}_t^k) = \mathbf{0}, \end{aligned} \quad (10)$$

Rearranging the terms to solve for \mathbf{W}_t yields the following closed-form solution:

$$(2\omega_t \alpha \mathbf{X}_t^T \mathbf{X}_t + \rho \mathbf{I}) \mathbf{W}_t = 2\omega_t \alpha \mathbf{X}_t^T \mathbf{F}_t^k + \rho \mathbf{Z}_t^k - \mathbf{Y}_t^k, \quad (11)$$

$$\begin{aligned} \mathbf{W}_t^{k+1} = & (2\omega_t \alpha \mathbf{X}_t^T \mathbf{X}_t + \rho \mathbf{I})^{-1} \\ & \times (2\omega_t \alpha \mathbf{X}_t^T \mathbf{F}_t^k + \rho \mathbf{Z}_t^k - \mathbf{Y}_t^k). \end{aligned} \quad (12)$$

b. **Update of \mathbf{F}_t :** With other variables fixed, the subproblem for \mathbf{F}_t is:

$$\begin{aligned} \min_{\mathbf{F}_t} & \left(\text{Tr}(\mathbf{F}_t^T \hat{\mathbf{L}}_t \mathbf{F}_t) + \alpha \|\mathbf{F}_t - \mathbf{X}_t \mathbf{W}_t^{k+1}\|_F^2 \right) \\ \text{s.t.} & \mathbf{F}_t^T \mathbf{F}_t = \mathbf{I}. \end{aligned} \quad (13)$$

Leaving $\mathbf{A}_t = \mathbf{X}_t \mathbf{W}_t^{k+1}$, the objective for \mathbf{F}_t becomes minimizing $f(\mathbf{F}_t) = \text{Tr}(\mathbf{F}_t^T (\hat{\mathbf{L}}_t + \alpha \mathbf{I}) \mathbf{F}_t) - 2\alpha \text{Tr}(\mathbf{F}_t^T \mathbf{A}_t)$. This is an optimization problem on the Stiefel manifold and lacks a closed-form solution. We solve it by employing a projected gradient descent approach, which involves iteratively taking a step in the negative gradient direction followed by a projection back onto the manifold to maintain orthogonality. The Euclidean gradient of $f(\mathbf{F}_t)$ is:

$$\nabla_{\mathbf{F}_t} f = 2(\hat{\mathbf{L}}_t + \alpha \mathbf{I}) \mathbf{F}_t - 2\alpha \mathbf{A}_t, \quad (14)$$

Starting with $\mathbf{F}_t^{(0)} = \mathbf{F}_t^k$, we perform a few inner iterations. In each inner iteration j , we first take a gradient descent step with a step size η :

$$\mathbf{F}_{\text{cand}}^{(j+1)} = \mathbf{F}_t^{(j)} - \eta \left((\hat{\mathbf{L}}_t + \alpha \mathbf{I}) \mathbf{F}_t^{(j)} - \alpha \mathbf{A}_t \right). \quad (15)$$

The resulting matrix $\mathbf{F}_{\text{cand}}^{(j+1)}$ is no longer guaranteed to be orthogonal. We enforce the constraint by projecting it back to the Stiefel manifold. This projection is achieved by finding the closest orthogonal matrix via Singular Value Decomposition (SVD). If the SVD of $\mathbf{F}_{\text{cand}}^{(j+1)}$ is $\mathbf{U} \Sigma \mathbf{V}^T$, the corrected orthogonal matrix is:

$$\mathbf{F}_t^{(j+1)} = \mathbf{U} \Sigma \mathbf{V}^T. \quad (16)$$

After a small number of such inner iterations, the final matrix is used as an update for the main ADMM loop, setting $\mathbf{F}_t^{k+1} = \mathbf{F}_t^{(j+1)}$.

Server-Side Update. The server, in turn, handles the global update for the consensus variable \mathcal{Z} :

$$\mathcal{Z}^{k+1} = \arg \min_{\mathcal{Z}} \left\{ \beta \|\mathcal{Z}\|_{S_p}^p + \sum_{t=1}^m \left(\text{Tr}((\mathbf{Y}_t^k)^T(-\mathbf{Z}_t)) + \frac{\rho}{2} \|\mathbf{W}_t^{k+1} - \mathbf{Z}_t\|_F^2 \right) \right\}. \quad (17)$$

By completing the square on the terms that involve \mathcal{Z} , the problem can be simplified as follows:

$$\mathcal{Z}^{k+1} = \arg \min_{\mathcal{Z}} \left\{ \beta \|\mathcal{Z}\|_{S_p}^p + \frac{\rho}{2} \|\mathcal{Z} - (\mathbf{W}^{k+1} + \frac{1}{\rho} \mathbf{Y}^k)\|_F^2 \right\}. \quad (18)$$

This problem has a closed-form solution given by the Tensor Singular Value Thresholding (TSVT) [35] algorithm.

2) *Dual Ascent Stage:* Finally, the dual variables \mathbf{Y} are updated through a gradient ascent step. This step leverages the primal residual $(\mathbf{W}_t^{k+1} - \mathbf{Z}_t^{k+1})$ to drive the local and global variables towards consensus.

$$\mathbf{Y}_t^{k+1} = \mathbf{Y}_t^k + \rho(\mathbf{W}_t^{k+1} - \mathbf{Z}_t^{k+1}), \quad (19)$$

where ρ serves as the step size for the dual ascent. The dual variable tensor \mathbf{Y} thus accumulates the degree of constraint violation, providing a corrective signal in subsequent iterations that drives the primal variables towards consensus and, ultimately, to the optimal solution.

C. Privacy and Security Considerations

A core design principle of our FMTTC framework is the preservation of data privacy at a fundamental level by avoiding the transmission of raw local data X_t . In our protocol, the only information transmitted from any client C_t to the server is its updated local model parameter, the projection matrix W_t^{k+1} .

Sharing W_t instead of X_t provides a significant privacy enhancement over centralized methods, as it only reveals abstract patterns learned from the data. However, we acknowledge that this approach does not offer formal privacy guarantees against sophisticated model inversion attacks that aim to reconstruct data from shared model parameters. Our framework should be viewed as providing a baseline level of privacy that is common in many federated learning systems. For applications requiring rigorous privacy guarantees, FMTTC could be integrated with advanced privacy-enhancing technologies such as differential privacy or secure aggregation in future work.

V. EXPERIMENTAL RESULTS

A. Experimental Settings

a) *Datasets:* To ensure a comprehensive evaluation of the proposed FMTTC framework, we conducted experiments on seven widely-used benchmark datasets: **WebKB4**, **20Newsgroups**, **Reuters**, **Keck**, **CORe50¹**, **BBC News²**, and **YALE**.

¹<https://vlomonaco.github.io/core50/index.html>

²<http://mlg.ucd.ie/datasets/bbc.html>

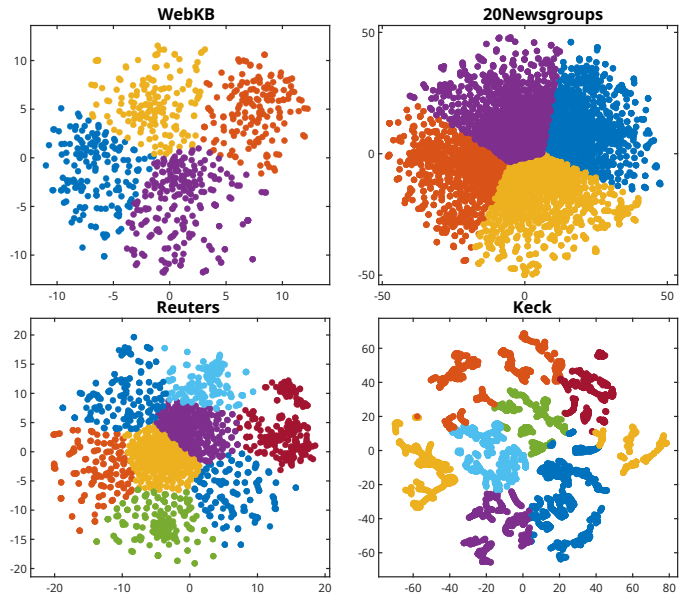


Fig. 3. t-SNE visualization of the WebKB, 20Newsgroups, Reuters, and Keck datasets. Each color represents a distinct class. The plots highlight the significant heterogeneity and complex, non-linearly separable structures within and across tasks (clients), motivating the need for a personalized and collaborative clustering approach like FMTTC.

These datasets span diverse modalities, ranging from high-dimensional sparse text documents to dense image vectors, allowing us to assess the method's versatility.

Crucially, to simulate a realistic cross-silo federated learning environment, we strictly follow a Non-IID data partitioning strategy. Instead of randomly shuffling data, we treat each natural data source as a distinct client (e.g., each university in WebKB4 or each news category in BBC acts as a client). This setting introduces significant statistical heterogeneity, as the data distribution varies across clients.

As exemplified by the t-SNE visualizations in Fig. 3 (WebKB, 20Newsgroups, Reuters, and Keck), the data points exhibit complex, non-linearly separable manifold structures. Moreover, the cluster boundaries differ visibly across tasks. This visualization underscores that a simple union of data or a single global model would fail to capture these fine-grained local structures, thereby motivating the need for our personalized clustering approach that can handle task-specific distributions while leveraging shared knowledge.

b) *Compared Methods:* To rigorously evaluate the effectiveness of FMTTC, we compare it against a comprehensive suite of baselines categorized into three groups. These methods are chosen to represent different levels of data access and collaboration strategies:

- **Single-Task Baselines (stSC, uSC):** These methods represent the two extremes of data usage. **Spectral Clustering (stSC)** [1] is trained independently on each client using only local data, serving as a baseline for the "isolated" scenario. Conversely, **Spectral Clustering-Union (uSC)** [1] centrally pools all data into a single dataset, ignoring the distribution shift between clients and the multi-task structure.
- **Centralized Multi-Task Clustering Methods (MBC,**

TABLE I

CLUSTERING PERFORMANCE COMPARISON ON VARIOUS DATASETS. ALL METRICS ARE IN PERCENT (%). THE BEST AND SECOND-BEST RESULTS ACROSS ALL METHODS ARE IN **RED BOLD** AND **BLUE BOLD**, RESPECTIVELY.

Dataset	stSC [1]			uSC [1]			MBC [36]			SMBC [37]			SMKC [37]		
	ACC	NMI	RI	ACC	NMI	RI	ACC	NMI	RI	ACC	NMI	RI	ACC	NMI	RI
WebKB4	63.37	21.44	62.45	63.76	20.75	62.56	62.22	18.86	60.19	67.05	28.87	66.40	60.09	12.06	59.98
20News	56.18	24.14	64.41	39.15	23.71	59.76	44.75	13.27	47.43	51.00	22.96	56.56	36.09	21.51	59.50
Reuters	85.17	66.54	81.87	79.36	57.85	78.73	75.71	57.79	75.71	85.03	68.24	82.40	69.93	37.68	69.12
Keck	50.04	48.80	83.25	47.32	44.85	82.60	35.43	25.98	83.95	37.95	28.63	84.24	41.84	31.08	84.57
core50	39.63	5.43	69.89	30.40	0.92	68.90	40.27	9.07	63.63	45.97	15.87	67.15	27.28	0.20	62.55
BBC News	54.78	28.32	74.17	55.02	34.49	75.10	68.17	58.58	82.29	70.35	56.48	82.99	74.22	60.09	84.87
YALE	24.12	24.37	22.62	27.64	20.06	30.92	34.48	30.64	35.16	36.20	39.94	38.68	45.33	41.15	44.82

Dataset	MTSC [38]			SFOMVC [39]			Fed-kmeans [10]			FedSpectral+ [40]			Ours		
	ACC	NMI	RI	ACC	NMI	RI	ACC	NMI	RI	ACC	NMI	RI	ACC	NMI	RI
WebKB4	76.86	45.72	67.42	73.65	32.42	57.62	54.54	15.91	38.95	50.86	14.90	61.12	78.11	46.04	74.28
20News	72.32	65.90	80.73	70.15	62.55	78.90	30.35	21.58	29.47	27.10	25.27	57.17	71.30	67.83	81.87
Reuters	77.89	56.09	73.00	76.50	54.20	71.80	69.37	44.17	66.98	28.19	15.14	61.51	89.40	73.85	86.23
Keck	43.87	38.85	83.85	48.22	40.15	82.50	23.89	23.27	58.11	51.06	42.91	81.57	56.72	57.68	85.64
core50	56.64	20.38	66.16	54.30	21.10	65.50	25.04	0.45	25.00	47.32	22.87	63.38	61.37	26.74	73.77
BBC News	76.67	63.67	84.90	75.50	62.90	83.80	22.96	26.97	24.36	55.13	22.22	78.76	77.90	63.81	85.34
YALE	54.10	32.47	61.65	52.80	33.50	60.10	21.55	18.21	20.04	49.81	35.06	55.19	60.35	48.12	67.28

SMBC, SMKC, MTSC: These algorithms assume unrestricted access to raw data from all tasks and typically serve as the performance upper bound. We include: **Multi-task Bregman Clustering (MBC)** [36], which minimizes an average Bregman divergence with task regularization; **Smart Multitask Bregman Clustering (SMBC)** [37], a transfer learning approach leveraging auxiliary data; **Smart Multi-task Kernel Clustering (SMKC)** [37], the kernelized variant of SMBC for non-linear structures; and **Multi-Task Spectral Clustering (MTSC)** [38], which explicitly captures task correlations via spectral analysis. Comparing against these methods validates whether FMTC can match centralized performance under privacy constraints.

• **Federated Clustering Methods (Fed-kmeans, FedSpectral+, SFOMVC, Ours):** These are the direct competitors in the privacy-preserving setting. **Federated K-Means (Fed-kmeans)** [10] aggregates local centroids; **Federated Spectral Clustering (FedSpectral+)** [40] aggregates Laplacian eigenvectors; and **Scalable Federated Orthogonal Multi-View Clustering (SFOMVC)** [39] handles multi-view data in federated settings. However, these methods typically employ a “one-model-fits-all” strategy or simple parameter averaging, often failing to account for the personalized manifold structures of heterogeneous clients. Our proposed **FMTC** addresses these limitations by learning personalized models while explicitly capturing inter-client correlations through tensor-based regularization.

c) *Evaluation Metrics.*: By following standard protocols in spectral clustering, we perform k-means on the normalized rows of the learned embedding matrices $\{\mathbf{F}_t\}$ to obtain discrete cluster assignments. To mitigate the sensitivity of k-means to initialization, we repeat the clustering process 10 times with different random seeds and report the result with the lowest minimal sum of squared errors. The clustering quality is

quantitatively evaluated with three standard metrics: Clustering Accuracy (ACC), Normalized Mutual Information (NMI), and Rand Index (RI) [41]. ACC is computed using the Hungarian algorithm to find the optimal one-to-one mapping between cluster assignments and ground-truth labels. Higher values of all three metrics indicate better clustering performance.

B. Experiment Results

The quantitative clustering results on all seven datasets are summarized in Table I. From the reported results, we have the following observations:

- **Compared with single-task spectral clustering methods**, our proposed FMTC can obtain more than 14.35, 20.74, 7.13 and 14.12 percent improvements on WebKB4, CORe50, Reuters and 20NewsGroups datasets in terms of Avg.ACC, respectively. It is because FMTC could utilize the relationships among multiple clustering tasks, whereas the single spectral clustering methods (i.e., stSC and uSC) implement each task independently or pool all data together while ignoring the multi-task structure. More specifically, on the highly heterogeneous 20NewsGroups dataset, FMTC achieves 71.30% in ACC, significantly outperforming stSC (56.18%) and uSC (39.15%). This demonstrates the effectiveness of capturing inter-client correlations in federated settings.
- **Compared with centralized multi-task clustering methods**, we could see that FMTC outperforms these competing methods in most cases despite not having direct access to raw data from all clients. This observation verifies the effectiveness of learning the latent cluster centers between each pair of spectral tasks and preserving the common embedded features across multiple clustering tasks. Notably, FMTC consistently outperforms MTSC, a centralized method with access to raw data. On the WebKB4 dataset, FMTC improves NMI

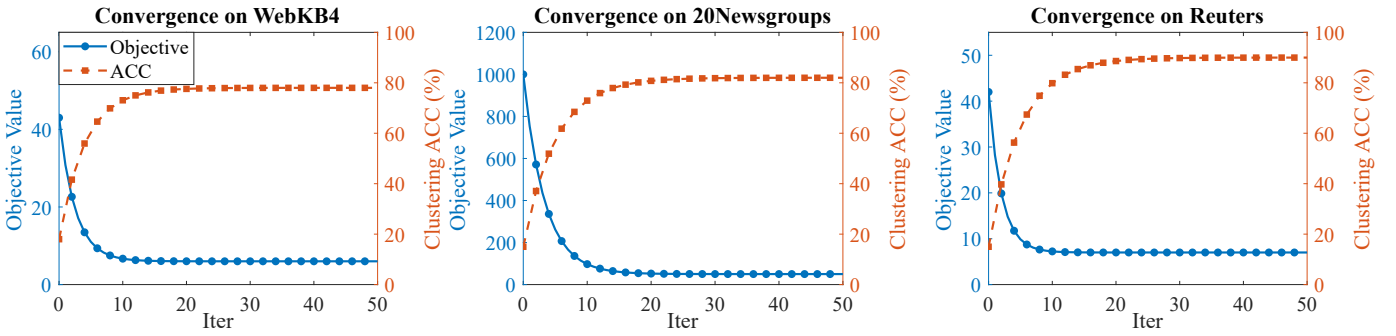


Fig. 4. Convergence analysis of our proposed FMTC framework on three datasets. For each dataset, we plot the overall objective function value and the average clustering ACC (%) versus the number of iterations.

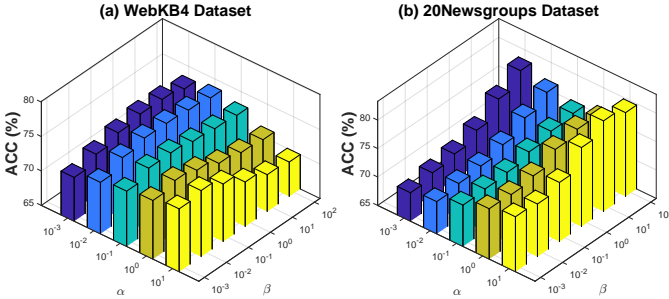


Fig. 5. Parameter sensitivity analysis of FMTC on the WebKB4 dataset. The figure shows the ACC (%) as a function of the collaboration weight β and the local fidelity weight α . Each row, corresponding to a specific α , is rendered in a unique color.

by approximately 0.32% over MTSC. This result empirically validates our hypothesis that the tensor low-rank regularization (Schatten p -norm) is more effective than traditional matrix-based regularization used in MTSC. Matrix-based methods can only capture pairwise task correlations by flattening the model structure, whereas FMTC explicitly captures the high-order, latent semantic relationships among tasks by organizing client models into a third-order tensor.

- **Compared with federated clustering methods**, FMTC significantly outperforms Fed-kmeans and FedSpectral+ across all datasets, particularly on highly heterogeneous data. For instance, on 20NewsGroups, Fed-kmeans and FedSpectral+ achieve only 30.35% and 27.10% accuracy, respectively, whereas FMTC achieves a substantial improvement to 71.30%. This drastic performance gap highlights a fundamental limitation of current federated clustering approaches: they typically rely on simple parameter averaging or centroid aggregation. In Non-IID scenarios where the underlying data distributions diverge significantly across clients, such averaging operations wash out the distinct manifold structures learned by local clients, leading to a collapsed global model that fits no one. In sharp contrast, FMTC maintains personalized projection matrices $\{\mathbf{W}_t\}$ for each client, preserving their unique local structures, while using the global tensor \mathcal{Z} only as a regularizer to guide the learning without enforcing strict homogeneity.

C. Convergence Analysis

We provide a rigorous theoretical proof of convergence for our algorithm in the appendix, which guarantees that the iterates converge to a KKT stationary point by leveraging established results for non-convex ADMM [42]. To complement this theoretical analysis and validate the practical effectiveness and stability of our proposed ADMM-based optimization algorithm, we visualize its convergence behavior on three representative datasets, WebKB4, 20NewsGroups and Reuters. Figure 4 plots the value of the overall objective function and the average clustering ACC against the number of iterations. As can be observed, the proposed FMTC framework exhibits excellent convergence properties across all tasks. In each case, the objective function value decreases monotonically and stationarity, stabilizing after approximately 15-20 iterations. Concurrently, the clustering ACC shows a steep increase in the initial iterations and then converges smoothly to a high-performance plateau. This fast and stable convergence demonstrates that our algorithm can efficiently find a high-quality solution in a limited number of communication rounds, making it practical for real-world federated learning scenarios.

D. Hyperparameter Sensitivity Analysis

To investigate the impact of our model's key hyperparameters, we analyze the performance sensitivity with respect to the local fidelity weight α and the global collaboration weight β on two representative datasets. The results are visualized in Fig. 5. The performance landscapes are shown to be complex and non-convex, with multiple ridges and local optima, reflecting the intricate interplay of the hyperparameters in real-world scenarios. For the WebKB4 dataset (Fig. 5a), a high-performance ridge is observed where the collaboration weight β is moderate (around 10^{-1} to 10^0). In contrast, the more complex 20Newsgroups dataset (Fig. 5b) exhibits a broader optimal region at a higher collaboration level ($\beta \approx 10^1$), suggesting a greater benefit from inter-task knowledge sharing. This demonstrates that while the optimal settings are dataset-dependent, the model is robust, maintaining strong performance across continuous regions rather than at sharp, isolated points. Importantly, for both datasets, performance consistently degrades as β approaches zero, empirically validating the necessity of our server-side tensorial correlation module.

TABLE II

COMPARISON OF IN-SAMPLE (IS) AND OUT-OF-SAMPLE (OOS) CLUSTERING PERFORMANCE (%). FOR EACH METHOD, OOS RESULTS ARE OBTAINED ON A HELD-OUT 20% TEST SET. THE GAP BETWEEN IS AND OOS PERFORMANCE INDICATES THE GENERALIZATION ABILITY. THE BEST AND SECOND-BEST RESULTS ACROSS ALL METHODS ARE IN **RED BOLD** AND **BLUE BOLD**, RESPECTIVELY.

Dataset	stSC [1]		uSC [1]		MBC [36]		SMBC [37]		SMKC [37]		MTSC [38]		Fed-kmeans [10]		FedSpectral+ [40]		Ours	
	IS	OOS	IS	OOS	IS	OOS	IS	OOS	IS	OOS	IS	OOS	IS	OOS	IS	OOS	IS	OOS
Metric: ACC (%)																		
WebKB4	63.37	49.43	63.76	49.10	62.22	46.67	67.05	53.64	60.09	43.26	76.86	62.26	54.54	40.36	50.86	35.60	78.11	64.67
20News	56.18	49.44	39.15	33.28	44.75	38.48	51.00	46.92	36.09	30.32	72.32	68.70	30.35	24.89	27.10	21.68	71.30	79.16
Reuters	85.17	78.36	79.36	72.22	75.71	68.14	85.03	79.93	69.93	61.54	77.89	72.44	69.37	61.74	28.19	22.55	89.40	85.27
Keck	50.04	33.53	47.32	31.23	35.43	23.03	37.95	25.81	41.84	27.61	43.87	31.13	23.89	15.77	51.06	34.21	56.72	47.64
core50	39.63	28.14	30.40	20.98	40.27	28.19	45.97	33.56	27.28	18.55	56.64	41.35	25.04	17.03	47.32	32.65	61.37	45.36
BBC News	54.78	48.21	55.02	47.87	68.17	59.31	70.35	62.61	74.22	65.31	76.67	69.77	22.96	18.83	55.13	46.31	77.90	74.40
Metric: NMI (%)																		
WebKB4	21.44	13.29	20.75	12.45	18.86	10.94	28.87	18.77	12.06	6.63	45.72	31.09	15.91	9.07	14.90	7.45	46.04	32.32
20News	24.14	19.31	23.71	18.49	13.27	9.95	22.96	18.83	21.51	16.35	65.90	56.67	21.58	16.18	25.27	18.20	67.83	60.19
Reuters	66.54	59.89	57.85	50.91	57.79	49.70	68.24	62.78	37.68	30.90	56.09	51.04	44.17	37.10	15.14	33.86	73.85	69.88
Keck	48.80	32.21	44.85	29.15	25.98	16.63	28.63	18.89	31.08	20.20	38.85	27.97	23.27	15.12	42.91	27.89	57.68	47.85
core50	5.43	3.53	0.92	0.55	9.07	5.80	15.87	10.47	0.20	0.11	20.38	14.06	0.45	0.28	22.87	15.32	26.74	8.82
BBC News	28.32	24.07	34.49	28.97	58.58	51.55	56.48	50.27	60.09	53.48	63.67	58.58	26.97	22.12	22.22	18.22	63.81	58.21
Metric: RI (%)																		
WebKB4	62.45	47.46	62.56	46.92	60.19	43.34	66.40	52.46	59.98	41.99	67.42	53.94	38.95	25.32	61.12	45.23	74.28	60.99
20News	64.41	57.97	59.76	52.59	47.43	40.32	56.56	52.04	59.50	51.17	80.73	78.31	29.47	23.58	57.17	48.60	81.87	71.30
Reuters	81.87	75.32	78.73	71.64	75.71	67.38	82.40	77.46	69.12	60.14	73.00	67.89	66.98	58.94	61.51	52.28	86.23	82.35
Keck	83.25	71.59	82.60	70.21	83.95	72.20	84.24	73.29	84.57	73.58	83.85	74.63	58.11	48.23	81.57	69.33	85.64	78.25
core50	69.89	60.10	68.90	58.56	63.63	53.45	67.15	57.75	62.55	52.54	66.16	58.22	25.00	19.50	63.38	54.51	73.77	69.89
BBC News	74.17	68.22	75.10	68.34	82.29	75.71	82.99	77.18	84.87	78.93	84.90	79.81	24.36	20.22	78.76	71.26	85.34	79.54

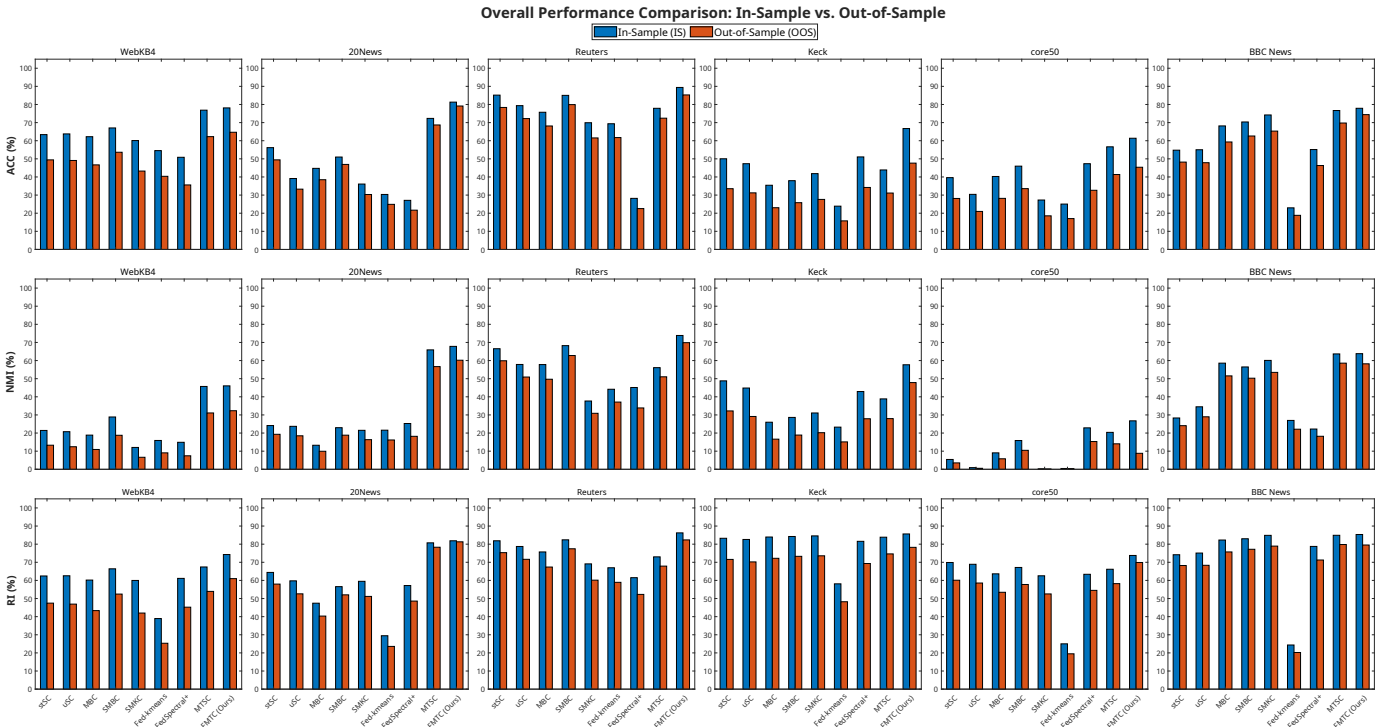


Fig. 6. Comprehensive comparison of In-Sample (IS) and Out-of-Sample (OOS) performance across all six datasets and three evaluation metrics (ACC, NMI, RI). Each subplot displays the performance of all nine competing methods on a specific task. The blue bars represent the performance on the training data (IS), while the orange bars represent the performance on the held-out test data (OOS). The gap between the blue and orange bars visually represents the generalization gap for each method. It is consistently observed that our proposed FMTC method not only achieves the highest performance but also exhibits one of the smallest generalization gaps, highlighting its superior robustness and ability to generalize to unseen data.

E. Out-of-Sample Extension Analysis

Existing methods that attempt to extend spectral clustering often resort to a disjoint "two-stage" approach: first generating pseudo-labels via clustering, and then training a separate classifier. As evidenced by the sharp performance drop of FedSpectral+ on unseen data (e.g., a drop of over 20% on

Reuters), this decoupled strategy suffers from severe error propagation—noise in the initial clustering is memorized by the classifier, leading to poor generalization. In contrast, FMTC demonstrates superior robustness with a minimal generalization gap. On the Reuters dataset, the OOS accuracy remains impressively high at 85.27%, significantly surpassing

all baselines. This success is attributed to our novel coupled optimization objective (Eq. 4). By simultaneously minimizing the spectral cut and the projection error $\|\mathbf{F}_t - \mathbf{X}_t \mathbf{W}_t\|_F^2$, we create a closed-loop system where the mapping function \mathbf{W}_t is not just a passive learner. Instead, it acts as a structural regularizer, forcing the spectral embeddings \mathbf{F}_t to lie in a subspace that is predictable by linear features. This "predictability constraint" effectively smoothes the learned manifold, preventing the model from overfitting to the idiosyncrasies of specific training points and ensuring that the learned structure is valid for the underlying data distribution. The ability to maintain high performance on OOS data confirms that our FMTC is ready for practical deployment. Once trained, the lightweight projection matrices $\{\mathbf{W}_t\}$ can be frozen and deployed on edge devices for real-time inference on streaming data, eliminating the need for frequent and costly model retraining.

VI. CONCLUSION

In this work, we present a Federated Multi-Task Clustering (*i.e.*, FMTC) model, a novel framework that addresses the dual challenges of intra-client correlation and inter-client correlation. The FMTC framework introduces two key components: client-side personalized clustering module and server-side tensorial correlation module. The client-side personalized clustering module integrates spectral embedding learning with parametric mapping function optimization into a unified closed-loop system, eliminating pseudo-label dependency and enabling out-of-sample inference. The server-side tensorial correlation module organizes local client models into a third-order tensor with low-rank regularization, explicitly capturing high-order shared knowledge while preserving personalized local structures. These two modules are jointly optimized via an efficient ADMM-based algorithm that ensures privacy preservation. Extensive experiments across seven benchmark datasets demonstrate that FMTC significantly outperforms state-of-the-art federated clustering algorithms, particularly in scenarios requiring strong generalization to unseen data. For future work, addressing the rotational ambiguity of learned projection matrices could further enhance performance.

REFERENCES

- [1] A. Y. Ng, M. I. Jordan, and Y. Weiss, "On spectral clustering: Analysis and an algorithm," *Adv. Neural Inf. Process. Syst. (NIPS)*, vol. 14, pp. 849–856, 2001.
- [2] R. Zhang, S. Hang, Z. Sun, F. Nie, R. Wang, and X. Li, "Anchor-based fast spectral ensemble clustering," *Inf. Fusion*, vol. 113, p. 102587, 2025.
- [3] Y. Feng, W. Liang, X. Wan, J. Liu, S. Liu, Q. Qu, R. Guan, H. Xu, and X. Liu, "Incremental Nyström-based multiple kernel clustering," in *Proc. AAAI Conf. Artif. Intell. (AAAI)*, vol. 39, no. 16, 2025, pp. 16613–16621.
- [4] Y. Zhao, Z. Bi, P. Zhu, A. Yuan, and X. Li, "Deep spectral clustering with projected adaptive feature selection," *IEEE Trans. Geosci. Remote Sens.*, 2025.
- [5] J. Williams and A. Robles-Kelly, "Spectral contrastive clustering," *Pattern Recognit.*, vol. 166, p. 111671, 2025.
- [6] B. McMahan, E. Moore, D. Ramage, S. Hampson, and B. A. y Arcas, "Communication-efficient learning of deep networks from decentralized data," in *Proc. Int. Conf. Artif. Intell. Statist. (AISTATS)*, 2017, pp. 1273–1282.
- [7] S. Han, S. Park, F. Wu, S. Kim, C. Wu, X. Xie, and M. Cha, "FedX: Unsupervised federated learning with cross knowledge distillation," in *Proc. Eur. Conf. Comput. Vision (ECCV)*, 2022, pp. 691–707.
- [8] M. Servetnyk, C. C. Fung, and Z. Han, "Unsupervised federated learning for unbalanced data," in *Proc. IEEE Global Commun. Conf. (GLOBECOM)*. IEEE, 2020, pp. 1–6.
- [9] H. H. Kumar, V. Karthik, and M. K. Nair, "Federated K-means clustering: A novel edge AI based approach for privacy preservation," in *Proc. IEEE Int. Conf. Cloud Comput. Emerg. Markets (CCEM)*. IEEE, 2020, pp. 52–56.
- [10] S. Garst and M. Reinders, "Federated K-means clustering," in *Proc. Int. Conf. Pattern Recognit. (ICPR)*. Springer, 2024, pp. 107–122.
- [11] D. Qiao, C. Ding, and J. Fan, "Federated spectral clustering via secure similarity reconstruction," *Adv. Neural Inf. Process. Syst. (NeurIPS)*, vol. 36, pp. 58 520–58 555, 2023.
- [12] A. Z. Tan, H. Yu, L. Cui, and Q. Yang, "Towards personalized federated learning," *IEEE Trans. Neural Netw. Learn. Syst.*, vol. 34, no. 12, pp. 9587–9603, 2023.
- [13] Y. Deng, M. M. Kamani, and M. Mahdavi, "Adaptive personalized federated learning," *arXiv preprint arXiv:2003.13461*, 2020.
- [14] D. Xie, Q. Gao, Y. Zhao, F. Yang, and W. Song, "Consistent graph learning for multi-view spectral clustering," *Pattern Recognit.*, vol. 154, p. 110598, 2024.
- [15] V. Garcia and A. Sanchez, "EPLSC: A new semi-supervised ensemble spectral clustering algorithm based on the graph P-laplacian for genetic data," *Adv. Eng. Intell. Syst.*, vol. 4, no. 01, pp. 102–113, 2025.
- [16] H. Zhang, J. Yang, B. Zhang, Y. Tang, W. Du, and B. Wen, "Enhancing generalized spectral clustering with embedding laplacian graph regularization," *CAAI Trans. Intell. Technol.*, 2024.
- [17] A. Rouhi, A. Bouyer, B. Arasteh, and X. Liu, "Two-pronged feature reduction in spectral clustering with optimized landmark selection," *Appl. Soft Comput.*, vol. 161, p. 111775, 2024.
- [18] W. Guo and W. Ye, "Deep spectral clustering via joint spectral embedding and K-means," in *Proc. IEEE Int. Conf. Syst. Man Cybern. (SMC)*. IEEE, 2024, pp. 3293–3299.
- [19] R. Presotto, G. Civitarese, and C. Bettini, "Federated clustering and semi-supervised learning: A new partnership for personalized human activity recognition," *Pervasive Mobile Comput.*, vol. 88, p. 101726, 2023.
- [20] C. Li, G. Li, and P. K. Varshney, "Federated learning with soft clustering," *IEEE Internet Things J.*, vol. 9, no. 10, pp. 7773–7782, 2022.
- [21] A. Ghosh, J. Chung, D. Yin, and K. Ramchandran, "An efficient framework for clustered federated learning," *IEEE Trans. Inf. Theory*, vol. 68, no. 12, pp. 8076–8091, 2022.
- [22] F. Sattler, K.-R. Müller, and W. Samek, "Clustered federated learning: Model-agnostic distributed multitask optimization under privacy constraints," *IEEE Trans. Neural Netw. Learn. Syst.*, vol. 32, no. 8, pp. 3710–3722, 2021.
- [23] Y. Zhang, H. Chen, Z. Lin, Z. Chen, and J. Zhao, "LCFed: An efficient clustered federated learning framework for heterogeneous data," in *Proc. IEEE Int. Conf. Acoust., Speech Signal Process. (ICASSP)*. IEEE, 2025, pp. 1–5.
- [24] Y. Zhang, Y. Zhang, Y. Lu, M. Li, X. Chen, and Y.-m. Cheung, "Asynchronous federated clustering with unknown number of clusters," *arXiv preprint arXiv:2412.20341*, 2024.
- [25] V. Yfantis, A. Wagner, and M. Ruskowski, "Federated K-means clustering via dual decomposition-based distributed optimization," *Franklin Open*, vol. 10, p. 100204, 2025.
- [26] W. Feng, Z. Wu, Q. Wang, B. Dong, Z. Tao, and Q. Gao, "Efficient federated multi-view clustering with integrated matrix factorization and K-means," in *Proc. Int. Joint Conf. Artif. Intell. (IJCAI)*, 2024, pp. 439–447.
- [27] Y. Zhang and Q. Yang, "A survey on multi-task learning," *IEEE Trans. Knowl. Data Eng.*, vol. 34, no. 12, pp. 5586–5609, 2022.
- [28] C. Huang, J. Huang, and X. Liu, "Cross-silo federated learning: Challenges and opportunities," *arXiv preprint arXiv:2206.12949*, 2022.
- [29] Y. Huang, L. Chu, Z. Zhou, L. Wang, J. Liu, J. Pei, and Y. Zhang, "Personalized cross-silo federated learning on non-iid data," in *Proc. AAAI Conf. Artif. Intell. (AAAI)*, vol. 35, no. 9, 2021, pp. 7865–7873.
- [30] J. Wen, Z. Wu, Z. Zhang, L. Fei, B. Zhang, and Y. Xu, "Structural deep incomplete multi-view clustering network," in *Proc. 30th ACM Int. Conf. Inf. Knowl. Manage. (CIKM)*. New York, NY, USA: ACM, 2021, pp. 3538–3542.
- [31] J. Xu, C. Li, Y. Ren, L. Peng, Y. Mo, X. Shi, and X. Zhu, "Deep incomplete multi-view clustering via mining cluster complementarity," in *Proc. AAAI Conf. Artif. Intell. (AAAI)*, vol. 36, no. 8, 2022, pp. 8761–8769.
- [32] J. Wen, Y. Xu, and H. Liu, "Incomplete multiview spectral clustering with adaptive graph learning," *IEEE Trans. Cybern.*, vol. 50, no. 4, pp. 1418–1429, 2020.

- [33] J. Wen, H. Sun, L. Fei, J. Li, Z. Zhang, and B. Zhang, “Consensus guided incomplete multi-view spectral clustering,” *Neural Netw.*, vol. 133, pp. 207–219, 2021.
- [34] J. Wen, Z. Zhang, Z. Zhang, L. Zhu, L. Fei, B. Zhang, and Y. Xu, “Unified tensor framework for incomplete multi-view clustering and missing-view inferring,” in *Proc. AAAI Conf. Artif. Intell. (AAAI)*, vol. 35, no. 11, 2021, pp. 10 273–10 281.
- [35] C. Lu, J. Feng, Y. Chen, W. Liu, Z. Lin, and S. Yan, “Tensor robust principal component analysis with a new tensor nuclear norm,” *IEEE Trans. Pattern Anal. Mach. Intell.*, vol. 42, no. 4, pp. 925–938, 2020.
- [36] J. Zhang and C. Zhang, “Multitask Bregman clustering,” *Neurocomputing*, vol. 74, no. 10, pp. 1720–1734, 2011.
- [37] X. Zhang, X. Zhang, and H. Liu, “Smart multitask Bregman clustering and multitask kernel clustering,” *ACM Trans. Knowl. Discov. Data*, vol. 10, no. 1, pp. 1–29, 2015.
- [38] Y. Yang, Z. Ma, Y. Yang, F. Nie, and H. T. Shen, “Multitask spectral clustering by exploring intertask correlation,” *IEEE Trans. Cybern.*, vol. 45, no. 5, pp. 1083–1094, 2015.
- [39] W. Feng, D. Liu, Q. Wang, W. Liang, and Z. Yan, “Scalable federated one-step multi-view clustering with tensorized regularization,” in *Proc. AAAI Conf. Artif. Intell. (AAAI)*, vol. 39, no. 16, 2025, pp. 16 586–16 594.
- [40] J. Thakkar and D. Joshi, “FedSpectral+: Spectral clustering using federated learning,” *arXiv preprint arXiv:2302.02137*, 2023.
- [41] C. D. Manning, *Introduction to information retrieval*. Syngress Publishing,, 2008.
- [42] Y. Wang, W. Yin, and J. Zeng, “Global convergence of ADMM in nonconvex nonsmooth optimization,” *J. Sci. Comput.*, vol. 78, no. 1, pp. 29–63, 2019.

APPENDIX

In this section, we provide the convergence analysis for Algorithm 1. The overall problem is non-convex due to the orthogonality constraint $\mathbf{F}_t^T \mathbf{F}_t = \mathbf{I}$ and potentially the tensor regularizer $\|\mathbf{W}\|_{S_p}^p$ (for $p < 1$). Our analysis follows the established framework for non-convex Alternating Direction Method of Multipliers (ADMM). We demonstrate that the sequence of iterates generated by Algorithm 1 converges to a Karush-Kuhn-Tucker (KKT) stationary point of the problem, provided the penalty parameter ρ is sufficiently large.

Our analysis relies on the following standard assumptions:

- A1.** (Bounded Objective) The objective function, comprising the local functions $f_t(\mathbf{W}_t, \mathbf{F}_t) = \omega_t(\text{Tr}(\mathbf{F}_t^T \hat{\mathbf{L}}_t \mathbf{F}_t) + \alpha \|\mathbf{F}_t - \mathbf{X}_t \mathbf{W}_t\|_F^2)$ and the global regularizer $g(\mathbf{Z}) = \beta \|\mathbf{Z}\|_{S_p}^p$, is proper, lower semi-continuous, and bounded from below.
- A2.** (Lipschitz Gradient) The smooth part of the objective function with respect to \mathbf{W}_t , denoted as $l_t(\mathbf{W}_t) = \alpha \|\mathbf{F}_t - \mathbf{X}_t \mathbf{W}_t\|_F^2$, has a Lipschitz continuous gradient. This is satisfied as l_t is a quadratic function. Let $L_t = 2\alpha \|\mathbf{X}_t^T \mathbf{X}_t\|_2$ be the Lipschitz constant, and let $L_f = \max_t L_t$.
- A3.** (Sufficient Decrease for \mathbf{F}_t -subproblem) The inexact Projected Gradient Descent (PGD) for the \mathbf{F}_t -subproblem is required to achieve a sufficient decrease in the Augmented Lagrangian. That is, there exists a constant $c_F > 0$ such that the update \mathbf{F}_t^{k+1} satisfies:

$$\begin{aligned} \mathcal{L}_\rho(\dots, \mathbf{F}_t^{k+1}, \dots) \leq & \mathcal{L}_\rho(\dots, \mathbf{F}_t^k, \dots) - \\ & \frac{c_F}{2} \|\mathbf{F}_t^{k+1} - \mathbf{F}_t^k\|_F^2. \end{aligned} \quad (20)$$

This is a standard condition for inexact solvers in non-convex optimization.

- A4.** (Bounded Augmented Lagrangian) We postulate there exists a penalty parameter $\rho_0 > 0$ such that for all $\rho \geq \rho_0$,

the Augmented Lagrangian \mathcal{L}_ρ is bounded from below over the sequence of iterates. This is a mild assumption given that the original objective function is bounded from below.

Note that the original assumption A3 regarding the full rank of $\mathbf{X}_t^T \mathbf{X}_t$ is not necessary. The strong convexity of the \mathbf{W}_t -subproblem is guaranteed by the quadratic penalty term $\frac{\rho}{2} \|\mathbf{W}_t - \mathbf{Z}_t^k\|_F^2$ for any $\rho > 0$, which makes the Hessian matrix $2\omega_t \alpha \mathbf{X}_t^T \mathbf{X}_t + \rho \mathbf{I}$ positive definite.

Under assumptions A1, A2', A3', and A4', if the penalty parameter ρ is sufficiently large, the sequence of iterates $\{\mathbf{W}^k, \mathbf{F}^k, \mathbf{Z}^k, \mathbf{Y}^k\}$ generated by Algorithm 1 has at least one limit point, and any limit point is a KKT point of the original problem.

Proof. The proof strategy is to reformulate our problem into a standard two-block non-convex optimization framework and then invoke established convergence results for ADMM applied to such problems.

1. Reformulation as a Two-Block Problem

The original problem can be cast as a two-block constrained optimization problem:

$$\min_{\mathbf{X}_1, \mathbf{X}_2} G(\mathbf{X}_1) + H(\mathbf{X}_2) \quad \text{s.t.} \quad \mathbf{A}\mathbf{X}_1 + \mathbf{B}\mathbf{X}_2 = 0, \quad (21)$$

where the blocks are defined as:

- **Block 1:** $\mathbf{X}_1 = (\mathbf{W}_1, \dots, \mathbf{W}_m, \mathbf{F}_1, \dots, \mathbf{F}_m)$.
- **Block 2:** $\mathbf{X}_2 = \mathbf{Z}$.
- **Block 1 Objective:** $G(\mathbf{X}_1) = \sum_{t=1}^m f_t(\mathbf{W}_t, \mathbf{F}_t)$, which is non-convex.
- **Block 2 Objective:** $H(\mathbf{X}_2) = g(\mathbf{Z})$, which is non-convex but admits an efficient proximal operator (TSVT).
- **Constraint:** The linear constraint $\mathbf{W}_t - \mathbf{Z}_t = 0$ for all t connects the two blocks.

Algorithm 1 is precisely an application of ADMM to this two-block problem, where the primal updates are performed sequentially for \mathbf{X}_1 (the client-side updates for \mathbf{W}_t and \mathbf{F}_t) and \mathbf{X}_2 (the server-side update for \mathbf{Z}).

2. Invoking Standard ADMM Convergence Theory

The convergence of ADMM for two-block non-convex optimization problems is well-established in the literature (e.g., Wang, Yin, and Zeng, 2019). These results typically show that if the algorithm’s parameters are chosen correctly, the sequence of iterates converges to a stationary point. The key requirements for these theorems to hold are:

- 1) The objective function is bounded from below (Assumption A1).
- 2) The smooth parts of the objective have Lipschitz continuous gradients (Assumption A2').
- 3) The subproblems for each block are solved to a sufficient degree of accuracy. In our case:
 - The \mathbf{W}_t -subproblem is solved exactly. Its objective is strongly convex with modulus ρ due to the penalty term, which guarantees a sufficient decrease of at least $\frac{\rho}{2} \|\mathbf{W}_t^{k+1} - \mathbf{W}_t^k\|_F^2$.
 - The \mathbf{F}_t -subproblem satisfies the sufficient decrease condition (Assumption A3').

- The \mathbf{Z} -subproblem is solved exactly via the proximal operator.

4) The penalty parameter ρ is sufficiently large. The specific condition is typically of the form $\rho > cL_f$ for some constant c , ensuring that the quadratic penalty dominates any potential increase caused by non-convexity.

Under these conditions, it can be proven that a carefully constructed Lyapunov function (often involving L_ρ and proximal terms related to the dual variable update) is monotonically non-increasing and bounded below. The convergence of this Lyapunov function implies that the difference between consecutive iterates converges to zero:

$$\lim_{k \rightarrow \infty} \|\mathbf{W}^{k+1} - \mathbf{W}^k\|_F = 0, \quad \lim_{k \rightarrow \infty} \|\mathbf{F}^{k+1} - \mathbf{F}^k\|_F = 0, \quad \text{etc.} \quad (22)$$

3. Verifying KKT Conditions at the Limit Point

The convergence of consecutive iterates allows us to establish the KKT conditions at any limit point $(\mathbf{W}^*, \mathbf{F}^*, \mathbf{Z}^*, \mathbf{Y}^*)$.

- **Primal Feasibility:** The dual update rule is $\mathbf{Y}_t^{k+1} - \mathbf{Y}_t^k = \rho(\mathbf{W}_t^{k+1} - \mathbf{Z}_t^{k+1})$. Since the sequence of iterates is bounded and the difference between consecutive iterates goes to zero, it can be shown that $\|\mathbf{Y}_t^{k+1} - \mathbf{Y}_t^k\|_F \rightarrow 0$. This implies that the primal residual converges to zero: $\lim_{k \rightarrow \infty} \|\mathbf{W}_t^{k+1} - \mathbf{Z}_t^{k+1}\|_F = 0$. Thus, at any limit point, $\mathbf{W}_t^* = \mathbf{Z}_t^*$, satisfying the primal constraint.
- **Stationarity:** The optimality conditions for the \mathbf{W}_t , \mathbf{F}_t , and \mathbf{Z} subproblems hold at each iteration $k+1$. For instance, the optimality condition for the \mathbf{Z} -update is $0 \in \partial g(\mathbf{Z}^{k+1}) - \mathbf{Y}^{k+1}$. As $k \rightarrow \infty$, since the iterates converge to a limit point, this becomes $0 \in \partial g(\mathbf{Z}^*) - \mathbf{Y}^*$. Combining the stationarity conditions from all subproblems at the limit point, along with primal feasibility, recovers the full KKT system of the original problem.

By leveraging the established convergence theory for non-convex two-block ADMM, we conclude that the sequence generated by Algorithm 1 converges to a KKT stationary point of the problem. \square



Gan Sun (Student Member, IEEE; Member, IEEE) is currently a Full Professor with South China University of Technology. He received the B.S. degree from Shandong Agricultural University in 2013, and the Ph.D. degree from the Shenyang Institute of Automation, Chinese Academy of Sciences in 2020. He was a Visiting Student with Northeastern University from April 2018 to May 2019, and the Massachusetts Institute of Technology from June 2019 to November 2019. He was an Associate Professor with the State Key Laboratory of Robotics, Shenyang Institute of Automation, Chinese Academy of Sciences, until 2024. He has authored papers in top-tier conferences such as CVPR, ICCV, ECCV, AAAI, IJCAI, and ICDM, as well as top-tier journals including TPAMI, TNNLS, TIP, TMM, TCSVT, and Pattern Recognition. His current research interests include lifelong machine learning, multitask learning, medical data analysis, domain adaptation, deep learning, and 3D computer vision.



Fazeng Li received the B.S. degree in Automation from South China University of Technology, China, in 2022, and the M.S. degree in Instrument Science and Technology from Wuhan University of Science and Technology, China, in 2025. He is currently pursuing the Ph.D. degree with South China University of Technology. His research interests include robotics, computer vision, and deep learning.



Xu Tang received the M.E. degree in Mechanical Engineering and Automation from the Harbin Institute of Technology, Harbin, China, in 2017. He is currently pursuing the Ph.D. degree in Software Engineering with the Dalian University of Technology, Dalian, China. His current research interests include computer vision and machine learning.



Qianqian Wang (Member, IEEE) received the B.Eng. degree from the Lanzhou University of Technology, Lanzhou, China, in 2014, and the Ph.D. degree in pattern recognition and intelligent systems from Xidian University, Xi'an, China, in 2019. She is currently an Associate Professor with the School of Telecommunications Engineering, Xidian University. She has authored or coauthored papers in top-tier journals and conferences such as the IEEE TPAMI, IEEE TNNLS, CVPR, and AAAI. Her research interests include dimensionality reduction, pattern recognition and deep learning.



Yang Cong (Senior Member, IEEE) received the B.Sc. degree from Northeast University in 2004, and the Ph.D. degree from the State Key Laboratory of Robotics, Chinese Academy of Sciences in 2009. He is currently a Full Professor with the School of Automation Science and Engineering, South China University of Technology, Guangzhou, China. He was a Research Fellow with the National University of Singapore (NUS) and Nanyang Technological University (NTU) from 2009 to 2011, and a Visiting Scholar with the University of Rochester. He has authored or coauthored over 100 technical papers in prestigious international journals and conferences, including the IEEE TPAMI, IEEE TNNLS, CVPR, NeurIPS, ICCV, and AAAI. His current research interests include computer vision, machine learning, lifelong learning, and medical image analysis. He serves on the editorial board of several journals.



Suyan Dai received his B.S. degree from the Shien-Ming Wu School of Intelligent Engineering, South China University of Technology, China, in 2024, where he is currently pursuing the M.S. degree with the School of Automation Science and Engineering. His research interests include robotics, reinforcement learning, and deep learning.